forensic sciences

MDPI

Article

Creation of an Experimental Animal Model for the Study of Postmortem Dark Scleral Spots

Matteo Nioi [1,*], Pietro Emanuele Napoli [2,3], Domenico Nieddu [1], Alberto Chighine [1], Maurizio Fossarello [2,4] and Ernesto d'Aloja [1]

[1] Forensic Medicine Unit, Department of Medical Sciences and Public Health, University of Cagliari, 09040 Cagliari, Sardinia, Italy; nieddu_domenico@hotmail.it (D.N.); alberto.chighine@unica.it (A.C.); ernestodaloja@gmail.com (E.d.)
[2] Department of Surgical Sciences, Eye Clinic, University of Cagliari, 09124 Cagliari, Sardinia, Italy; pietronapoli@ymail.com (P.E.N.); maurizio.fossarello@gmail.com (M.F.)
[3] Studio Oculistico Dr. Pietro Emanuele Napoli, 09014 Carloforte, Sardinia, Italy
[4] Studio Oculistico Dr. Maurizio Fossarello, 09128 Cagliari, Sardinia, Italy
* Correspondence: nioimatteo@gmail.com; Tel.: +39-349-086-8477

Abstract: Postmortem dark scleral spots, first described by Sommer in 1833, are well-known in forensic pathology. **Background/Objectives:** Despite this, their presence is currently considered a nonspecific sign, and their pathogenesis has received little attention in forensic literature. In recent years, however, preliminary studies have suggested new mechanisms in their pathogenesis and links to specific types of death. This study aims to create an experimental model for studying scleral spots. **Methods:** Twenty sheep, already slaughtered for food, were used. After decapitation, the heads were transported to a room with known temperature and humidity. The right eye underwent eyelid excision, while the left eye's eyelids were sutured. Continuous observation for approximately 24 h was conducted, with brief interruptions to observe the closed eyes. **Results:** Dark scleral spots appeared in all open eyes (20/20) after an average of 240.96 ± 58.36 min. The spots did not appear in any of the closed eyes. **Conclusions:** Experimental data indicate that despite the different location compared to human cadavers, this model serves as an excellent experimental framework for studying postmortem scleral spots.

Keywords: postmortem scleral spots; postmortem tache noire; forensic ophthalmology; eye postmortem; ocular surface; sclera; animal models; sheep model; ovine model in eye research; postmortem optical coherence tomography

Citation: Nioi, M.; Napoli, P.E.; Nieddu, D.; Chighine, A.; Fossarello, M.; d'Aloja, E. Creation of an Experimental Animal Model for the Study of Postmortem Dark Scleral Spots. *Forensic Sci.* **2024**, *4*, 487–498. https://doi.org/10.3390/forensicsci4040032

Academic Editors: Emmanouil I. Sakelliadis and Sorin Hostiuc

Received: 8 August 2024
Revised: 12 September 2024
Accepted: 20 September 2024
Published: 24 September 2024

1. Introduction

Postmortem dark scleral spots (PDSSs), or 'tache noire', were first documented by Sommer in 1833. [1] These spots appear as brown to black discolorations on the scleral surface of cadavers, typically taking on a vaguely band-like shape during the early postmortem interval. Historically, PDSSs have been considered a nonspecific sign, observed when the eyelids remain open postmortem, exposing the sclera to air.

Tache noire forms due to postmortem drying of the sclera when the eyes remain open after death, leading to a brownish-black, and sometimes reddish, band-like discoloration.

The drying effect is more pronounced when eyes are open, causing rapid evaporation from the ocular surface.

PDSSs can manifest relatively early after death. When the eye remains open postmortem, the entire ocular surface undergoes a dehydration process. In the cornea, this phenomenon leads to early thinning with alterations in the tissue's three-dimensional structure, which, in later postmortem intervals, results in tissue opacification. The sclera is also not immune to dehydration-related changes: in the area exposed to air (generally the portion located medially or laterally to the cornea), discoloration occurs within 1–2 h.

Initially, these discolorations are described as yellowish, then turn yellowish-brown, and eventually black. The evolution of tache noire starts with the formation of yellowish discolorations that progress to yellowish-brown or sometimes reddish and finally to black as desiccation continues. The process is influenced by environmental factors such as air movement, temperature, and humidity, which can accelerate or decelerate the drying process. The eyeball itself loses tension due to the hypostasis of transcellular liquids, contributing further to the formation and evolution of the discoloration. Tache noire typically appears as band-like discolorations located on both sides of the cornea, where the conjunctiva is exposed to air. The specific shape and extent of the discoloration are determined by the degree of exposure and the environmental conditions. These markings are distinct and localized to the areas not covered by the eyelids.

However, it is the practical experience of every forensic pathologist that mere exposure of the eye to ambient air, when an individual dies with their eyes open and this condition persists postmortem, is not sufficient to cause the formation of PDSSs [2–7].

Recently, some preliminary studies have focused on PDSSs, providing new insights from an epidemiological, morphological, and thanatogenesis perspective.

Regarding epidemiology, a study on a sample of 905 cases revealed the presence of PDSSs in only 21 cases (2.3%). The same epidemiological investigation showed that the phenomenon was bilateral in 71% of the cases and unilateral in only 29%. The most significant finding, however, concerned the cause of death: the data indicated that the manifestation of PDSSs was essentially linked to three main dynamics. In 33.3% of the cases, it was due to violent mechanical asphyxiation from hanging; in another 33.3%, it was caused by hemorrhagic shock; and in the remaining 33.3%, death resulted from cranial-encephalic trauma [8].

Further preliminary studies on the pathogenesis of PDSSs have highlighted that, in addition to dehydration, choroidal detachment at the site of spot formation may be a contributing factor to the phenomenon [9,10].

Preliminary studies suggest that, contrary to previous beliefs, PDSSs may not be merely a nonspecific sign resulting from the dehydration of the ocular surface. Instead, they could provide valuable information not only on the postmortem interval (PMI) but also on the cause of death. Despite these new findings, very few studies, especially in the modern era, have considered the significance of this sign, its pathogenesis, and its practical utility. This gap in research is primarily due to the rarity of the sign, which occurs in a small percentage of cadavers where death resulted from hemorrhagic shock, violent mechanical asphyxia by hanging or cranial trauma, with the eyes remaining open postmortem, exposing the sclera to dehydration. Additionally, there is the challenge of studying such a delicate tissue in humans, particularly when cadavers must be returned to their families after forensic activities are completed. However, the emergence of these new insights necessitates further investigation into this sign, the observation of which could have significant implications for forensic practice.

The aim of this work is to create an experimental animal model to study PDSSs, considering the potential practical implications of preliminary data.

2. Materials and Methods

2.1. Choice of the Animal Model

The selection of the animal model involved reviewing existing literature, particularly focused on the ocular surface.

To date, various types of animals, such as mice, rabbits, pigs, primates, and dogs, have been used to create models for studying the eye [11–14].

In recent years, however, different models have been used, such as the ovine model, which offers advantages like the size of the eye and the similarity of the tissue to that of humans, making it particularly useful in studying transplant reactions and eyelid surgery [15–18].

Sheep and human eyes differ anatomically due to their distinct evolutionary needs. In sheep, the eyes are positioned laterally on the sides of the head, providing a panoramic field of vision crucial for detecting predators. The lateral placement and pronounced orbital ridges protect and stabilize the eyes during grazing.

In contrast, human eyes are positioned at the front of the skull with deeply set orbits surrounded by a robust bony structure. This structure allows for a wide range of eye movements, enhancing the ability to focus accurately on specific objects. Sheep eyes, approximately 30% larger than human eyes, are frequently used in ocular research due to their anatomical similarities. The larger size (approximately 30 mm in vertical diameter compared to 23 mm in humans) facilitates surgical interventions and allows for the collection of larger samples of aqueous and vitreous humor, as well as corneal tissue. Moreover, sheep possess a third eyelid, or nictitating membrane, which humans do not have. This membrane plays a crucial role in protecting the eye and keeping it moist by spreading the tear film. Another significant difference is the shape and size of the pupil. Sheep have horizontal, rectangular-shaped pupils, which are particularly effective for scanning the horizon and maintaining a wide field of view—an essential adaptation for detecting predators. In contrast, humans have round pupils, which are optimized for focusing light directly onto the retina, enhancing detailed vision and depth perception. At the histological level, the sheep retina has a higher proportion of rods compared to cones, while the human retina is densely packed with cones, especially in the fovea. The cornea in sheep is thicker and more robust than in humans, providing additional structural support. Additionally, sheep possess a tapetum lucidum, a reflective layer behind the retina, which is absent in humans. The sclera in sheep is thicker, and the arrangement of extraocular muscles differs, reflecting structural adaptations to their respective environments. The sclera, particularly in the peripapillary region, exhibits structural characteristics—especially concerning the distribution of collagen fibers—that are similar across all mammals, including sheep. In ovines, the hydration of the ocular surface is managed differently than in humans. Sheep have a thicker cornea and a nictitating membrane (third eyelid), which aids in protecting and maintaining moisture on the eye's surface [19–22].

This type of model, specifically for the purposes of the current study, offered several advantages beyond the anatomical and general ones already mentioned. First, there is the ample availability in our region and the practical possibility of observing multiple samples within a short timeframe. Second, the large size of the eye, both overall and relative to the head, allowed for more accurate observation compared to models where the eye was small or where a large eye was associated with a proportionately large head, making transport difficult. Third, a recent study has investigated the adhesion forces between the nervous structure and the vitreous (which could play a role in the formation of PDSSs), demonstrating significant similarities between humans and sheep. This finding is particularly relevant to the type of experiment we are planning to conduct [23]. Fourth, in our region, sheep heads are not used for food purposes after decapitation and are considered waste material. It is worth noting that obtaining this material from a public slaughterhouse ensures that, from an ethical standpoint, all procedures comply with current legislation and European laws regarding animal welfare [Council Regulation (EC) No. 1099/2009 of 24 September 2009 on the protection of animals at the time of killing]. For this reason, not only is it possible to obtain more samples at low cost, but since the animals are already destined for slaughter for food use, no additional ethical approval is required. Lastly, but no less importantly, our group has already conducted studies on this model involving different tissues and biofluids (cornea, aqueous humor, and vitreous humor) from anatomical, imaging, and chemical–physical perspectives in the postmortem context. For this reason, a deeper understanding of the model provides us with greater tools to explain any unexpected postmortem phenomena.

2.2. Description of the Experimental Procedure

Twenty-two heads of young adult female sheep (*Ovis aries*), aged 24–48 months and having passed standard food consumption controls, were obtained from a local slaughterhouse (CO.AL.BE. dei F.lli Contu & C. s.n.c. Selargius, Cagliari, Sardinia, Italy).

The animals were sacrificed by jugular vein incision following electrical stunning and then decapitated according to standard meat processing protocols. Multiple operators performed the procedure simultaneously, allowing the slaughter of seven animals at a time. The process involves several stages: transporting the animals to the slaughter room, stunning them to reduce suffering, severing the jugular vein, bleeding, and decapitation.

Subsequently, each head was placed in a plastic bag with the eyes closed to avoid abrasions to the sclera or blood contamination during transport. The entire procedure took approximately 15 min per animal. The transport from the slaughterhouse to the morgue was carried out in three phases, comprising two groups of 7 heads and one group of 6. The latency between death and the start of the observation period was approximately 35 min for all the animals.

Therefore, during the first 35 min, all eyes were kept closed. The heads were transported for preparation to a room in the morgue where there were no airflows, and the conditions of lighting, humidity, and temperature were known and stable. Specifically, the lighting followed the standards set by Italian legislation for autopsy rooms (300 lux for general lighting, 10,000 lux for the area around the autopsy table, and 100,000 lux on the autopsy table). Humidity, monitored by a hygrometer, remained constant at 45% throughout the experiment. The average temperature was 21.5 $\pm$ 0.7 °C for the entire duration of the experiment.

Upon arrival at the morgue, the right eye of each head was kept open by surgically removing all three eyelids using a cold-blade scalpel. An incision was made in the periorbital skin approximately two centimeters from the bony orbital margins, extending to the lower edge of the palpebral conjunctiva. The third eyelid (present in sheep but not in humans) was also removed to maximize air exposure.

In contrast, the other eye was kept closed using an adhesive patch, which could be removed to allow for observation

The heads were divided into different groups according to their position for observation. Specifically, 10 heads were placed in a natural position with the cut surface resting on the table. The others were positioned using a special cardboard support following these orientations: 2 heads with the snout facing down, 2 heads with the snout facing up, 2 with the open eye facing up, 2 with the open eye facing down, and 2 with the top of the head resting on the support (Figure 1).

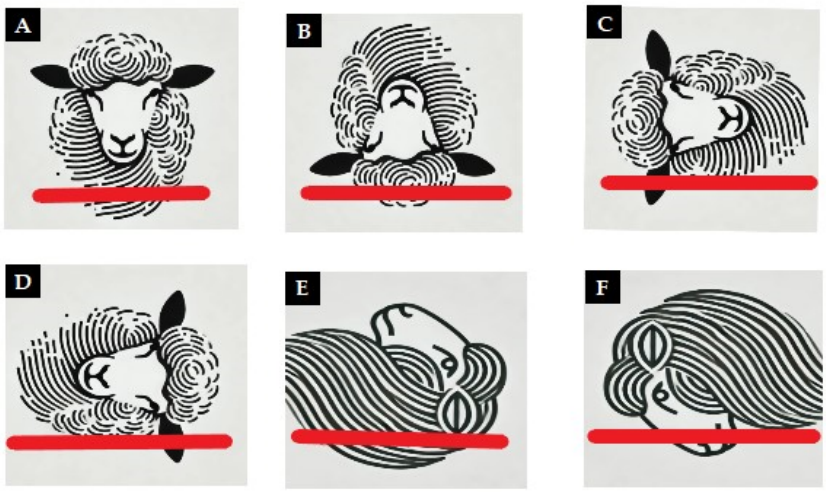

Figure 1. The panel shows the various positions of the heads during observation at the morgue. The red line represents the supporting surface, made of cardboard, arranged so that both eyes were exposed to

the ambient air. The different positioning in space was aimed at determining whether the position assumed by the head postmortem and the resulting arrangement of the tissues and intraocular fluids could influence or alter the appearance of PDSSs. In (**A**), the head is shown in a natural position with the cut surface resting on the support. In (**B**), the configuration shows the cut surface facing upward with the top of the head resting on the cardboard. In (**C**), the head is placed on its right side with the ipsilateral (open) eye facing downward and the left (closed) eye facing upward. In (**D**), the head is positioned on its left side with the ipsilateral (closed) eye facing downward and the right (open) eye facing upward. In (**E**), the sheep's snout is facing upward. In (**F**), the snout is facing downward.

Continuous observations, supplemented with photographs, were conducted by three operators for the first 12 h to identify the onset of scleral discoloration. Subsequent observations were made at intervals of 2 h from 14th to 24th hour to identify the onset of the full manifestation of the sign in its typical form (dark brown color).

The confirmation that the observed spots were postmortem scleral discolorations and not due to other phenomena was carried out through a single optical coherence tomography (OCT) scan (iVue SD-OCT, Optovue Inc., Fremont, CA, USA) performed during the first observation of the PDSSs.

Confirmation using a portable OCT programmed for ocular surface scans was performed in two stages for each sample. The first scan was conducted at the initial manifestation of scleral discoloration, and the second scan was performed when the spot had developed the characteristic black-brown coloration. As the device was a portable OCT, the examination was carried out in situ by moving the instrument within the observation room with minimal movement of the head to facilitate the examination.

The images were evaluated by ophthalmology specialists experienced in OCT, who assessed the condition of the eye during the experiment and reported the presence of any alterations.

3. Results

The protocol employed allowed the detection of scleral spots in all 20 eyes (100%) kept open through eyelid excision. In contrast, the appearance of scleral spots was not detected in any of the eyes kept closed using adhesive support. This evidence is compelling, making statistical analysis unnecessary. However, some chronological and morphological parameters have been examined and will be reported below.

3.1. Timing

The manifestation of the initial discoloration occurred in all samples with the eye open at an average interval of 223.5 $\pm$ 53.75 min postmortem. The full manifestation of the sign was verified at an average of 817.65 $\pm$ 401.74 min postmortem (Table 1).

Table 1. The table describes, for each sample, the following details: In the left column, the postmortem interval, in minutes, at which discoloration of the sclera began and was macroscopically appreciable; in the right column, the time of observation at which the scleral spot assumed its characteristic dark brown to blackish coloration.

Samples	Time of Initial Discoloration Manifestation in the Right Open Eye (Minutes)	Time of Full Dark Sign Manifestation in the Right Open Eye (Minutes)
Sample 1	162	529
Sample 2	186	349
Sample 3	202	567
Sample 4	183	1080
Sample 5	213	568
Sample 6	233	350
Sample 7	161	1440
Sample 8	187	351

Table 1. *Cont.*

Samples	Time of Initial Discoloration Manifestation in the Right Open Eye (Minutes)	Time of Full Dark Sign Manifestation in the Right Open Eye (Minutes)
Sample 9	195	570
Sample 10	197	570
Sample 11	178	573
Sample 12	195	575
Sample 13	273	1440
Sample 14	299	1440
Sample 15	275	1320
Sample 16	357	1200
Sample 17	273	576
Sample 18	236	577
Sample 19	289	1080
Sample 20	176	1200
Mean	223.5	817.65
Standard deviation	53.75	401.74

Macroscopically, the evolution of the sign is characterized by an initial period during which the sclera appears completely white upon observation. Starting from the 2nd hour postmortem, a discoloration begins to manifest, becoming increasingly intense and reaching its peak in 100% of cases by the 24th hour postmortem (Figure 2).

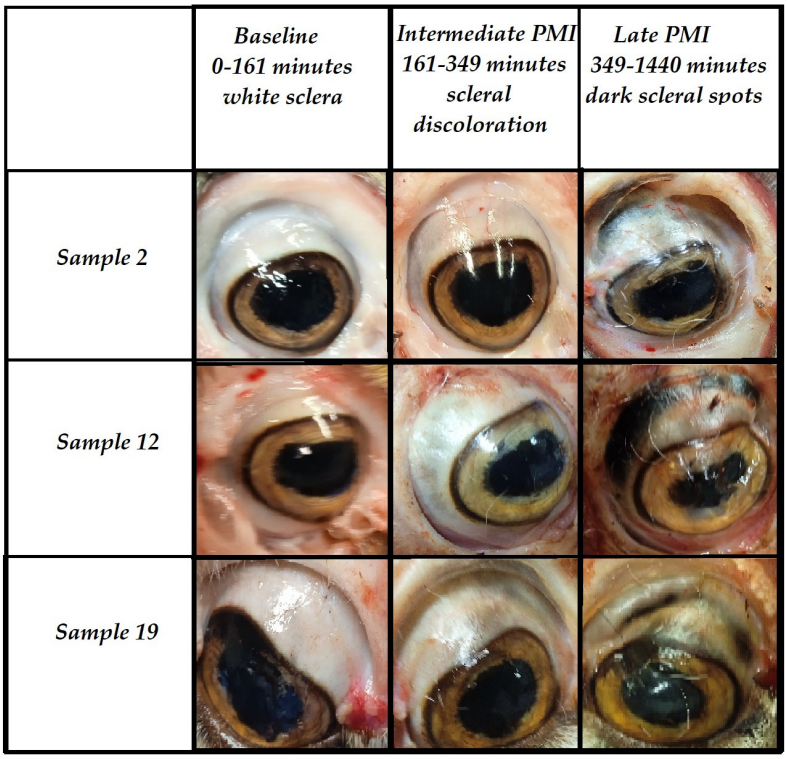

Figure 2. The figure shows the macroscopic characteristics of the eye at baseline (0–161 min postmortem), in an intermediate PMI (161–349 min—scleral discoloration), and in a late PMI (349–1440 min—dark scleral spot.

3.2. Morphology

Upon initial detection of scleral discoloration, an OCT scan was performed. In 100% of early observations, the data revealed a morphology characterized by detachment between the scleral layer and the choroid, consistent with previous studies [8–10].

In the later stages, as the sign fully manifested, choroidal detachment was accompanied by significant scleral dehydration and delamination (Figure 3).

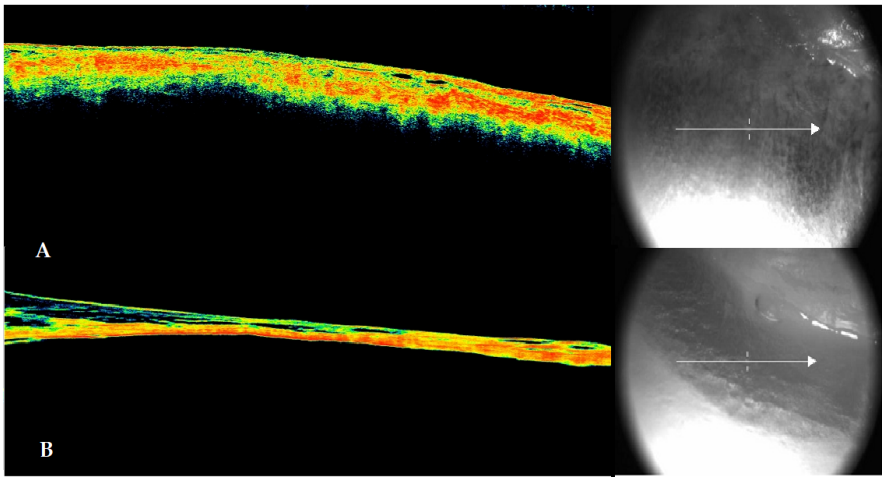

Figure 3. The figure shows in panel (**A**) the morphological configuration of the scleral discoloration highlighted through OCT (left side) and the corresponding infrared section (right side), with the arrow indicating the direction of the cross-section. A detachment between the sclera and choroid, as well as initial dehydration of the ocular surface, are evident. In panel (**B**), the OCT scan configuration of the dark brown to blackish scleral spot that appeared in the later postmortem intervals is shown. The color scale in the OCT images reflects tissue reflectivity: red indicates high reflectivity, yellow indicates medium-high reflectivity, and green to dark areas indicate lower reflectivity. Both the advanced dehydration of the ocular surface and the clear detachment between the sclera and vitreous (which appears less dense due to probable liquefaction) are evident. The sclera appears delaminated at several points in the inner layers of the tunic.

Another notable finding regarding morphology is the location where PDSSs manifested in our model. While scleral spots in humans typically appear at the equator of the eyeball (i.e., 3 o'clock and 9 o'clock positions), in the experimental model, the appearance was predominantly observed in the upper quadrant (9 o'clock to 12 o'clock positions). Surprisingly, the localization of the spots was not influenced by the positioning of the head in space. In fact, the spots were predominantly found in the supero-lateral quadrants (9–12). Only in three out of twenty cases (15%) where the head was maintained in a natural position were these portions of the sclera not involved (Figure 4).

Additionally, the shape of the spot is not band-like, as in human cadavers, but rather appears vaguely ribbon-like and semicircular.

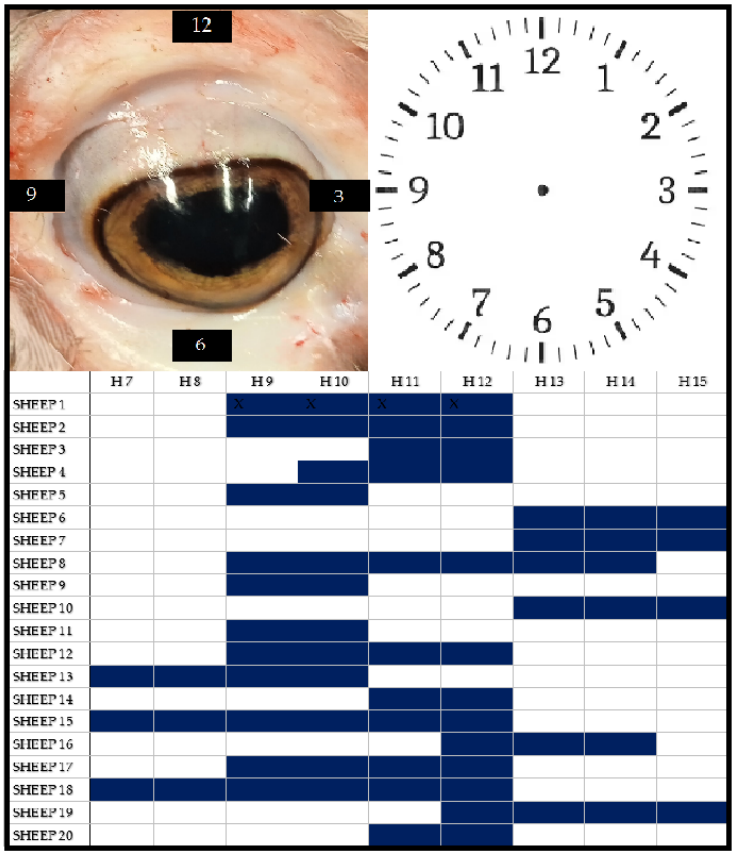

Figure 4. In the upper part of the figure, on the left, there is a photo of a sheep's eye, and on the right, the schematic representation of the ocular portions of the sclera based on the classic 'clock-face' scheme used in clinical practice. The lower part of the figure shows, in blue, the location of the PDSSs for each examined sample.

4. Discussion

The aim of the current study was to create an animal model through which to study PDSSs. The results show that, through the proposed model, it is possible to achieve the manifestation of PDSSs in all cases subjected to the experimental procedure.

The study also confirmed that postmortem dehydration of the ocular surface exposed to air is necessary, though not sufficient, for the manifestation of the sign. PDSSs did not appear in any eyes that were kept covered by the eyelid. Postmortem, particularly in the first few hours, if the eye is exposed to air (regardless of temperature), rapid evaporation and drying occur in the superficial layers of the exposed ocular surface [24–27].

Dehydration is further promoted by the cessation of homeostatic mechanisms postmortem, which normally maintain ocular surface hydration. Specifically, there is a complete cessation of tear film production, and profound alterations occur in both the aqueous humor and vitreous humor. These changes impact the chemical composition of these biofluids and, consequently, the characteristics of the ocular surface. Numerous studies have demonstrated that alterations in the ocular surface are accompanied by chemical and physical changes within the eye, which become more pronounced with the increase of the postmortem interval. The aqueous humor undergoes slow and progressive evaporation, resulting in alterations to the shape of the corneal surface. Within the aqueous humor, cellular aggregates can be detected, which are indicative of the desquamation of the corneal endothelium and the structure of the anterior chamber. Conversely, the vitreous humor undergoes progressive liquefaction, leading to a physical state change from gelatinous to liquid. While such alterations are clearly visible in the cornea, which requires a high degree

of transparency for its lens function, they also affect the sclera, although to a lesser extent in terms of macroscopic detectability [26,27].

The results of this study, in addition to recreating PDSSs in an animal model, have confirmed several elements crucial for understanding the thanatogenesis of the sign. Of significant importance is the confirmation that, in all samples examined morphologically and through imaging, a choroidal detachment was found corresponding to the scleral spot.

This alteration, when the sclera undergoes extensive dehydration, primarily results in the thinning of the overlying scleral portion. The thinning of this structure, in addition to a change in color due to the superficial dehydration of the tissue and conjunctiva, causes the translucency from the thinning to reveal the underlying layer, the choroid, which is blackish in color. This layer is normally invisible under physiological conditions and, in humans, only becomes apparent due to certain pathological conditions, such as connective tissue disorders, giving the scleral surface a bluish tint. Postmortem, the absence of compensatory homeostatic mechanisms results in this phenomenon manifesting in areas with significant exposure to the environment or physiologically thinner regions, which is inextricably linked to the detachment of the choroid. As recent postmortem studies have shown, the movement of molecules and fluids through ocular structures occurs along a gradient, contributing to tissue alterations that can be macroscopically observed [28–33].

The study data further confirm that PDSSs manifest when the cause of death, as in our animal model, is hemorrhagic shock.

Despite the fact that every forensic pathologist has likely encountered PDSSs at some point in their career, surprisingly, literature on the phenomenon is scarce. The lack of interest is primarily due to the inconsistency of the sign, which is considered nonspecific because not all cadavers with open eyes postmortem exhibit the tache noire. However, when the analysis is restricted to cases where PDSSs are present, some preliminary studies have indicated that the causes of death are primarily attributable to three mechanisms: mechanical asphyxia by hanging, cranial trauma, and hemorrhagic shock. From a pathophysiological perspective, although the dynamics leading to these types of death are quite different, they share a common feature: a sudden change in intraocular pressure during the perimortem period (either positive or negative), potentially capable of causing a choroidal detachment [8,9]. This finding, which still requires further epidemiological investigation with large-scale data, if confirmed, could become an important tool for forensic pathologists in the differential diagnosis of the cause of death.

In the analysis of the results, it is important to highlight some differences compared to the sign commonly observed in routine forensic pathology practice, as well as from empirical observations in some specialized books, given that very few experimental studies have analyzed PDSSs.

The variations mainly involve the timing of spot formation, the morphological evolution of the sign, and the location of the spots. These can be attributed to the anatomical peculiarities of the ovine eye compared to the human eye (larger size, greater thickness, different orbital shape, and the presence of a third eyelid) and the deliberate maximization of dehydration exposure, which affected the entire ocular globe rather than just a portion of the sclera.

Regarding the timing of the sign's appearance, while PDSSs are expected to appear within 60–120 min in humans, the current study revealed that the sign manifested after approximately 223.5 $\pm$ 53.75 min in the described model [3]. This difference in the timing of appearance can be primarily attributed to the anatomical differences between ovine and human eyes, both in terms of size and ultrastructural characteristics. These differences, although relatively modest, may play a role in the delayed manifestation of the sign in our model [28–30].

Similarly, regarding the evolution of the sign over time, our model did not exhibit the phase where the portion of the sclera, which later underwent discoloration and the formation of PDSSs, showed a yellowish tint due to dehydration. In the examined samples, as previously mentioned, the progression moved directly from discoloration to the

formation of spots without other macroscopic manifestations. This phenomenon can also be attributed to the differences in the ocular structure between humans and sheep.

Finally, concerning the portion of the sclera where the sign appeared, the effect can be attributed to various factors. Besides the anatomical characteristics (particularly the different adherence between the vitreous body and the choroid), the type of model used in the protocol, which aimed to maximize the dehydration effect on the entire ocular globe, certainly played a role. This approach resulted in extensive air exposure to areas of the globe that are usually covered by the eyelids, promoting early dehydration.

The study revealed that in this model, the spatial localization of the spots is not influenced by the head's position. The results showed a predominant involvement of the supero-lateral quadrants (85%), which, in open eyes, were unaffected by the spots in only 3 out of 20 cases (15%).

Despite differences observed compared to forensic practice, the proposed model successfully reproduced a sign that is rare in real cases. This sign could hold greater significance than currently reported in the literature, both for estimating the postmortem interval (PMI) and determining the causes of death. The data currently available are limited and fragmented. To gain a better understanding of the sign and apply the findings in practice, further studies are needed, primarily using animal models. These studies should analyze the phenomenon with a greater number of samples using OCT, as well as employ different methodologies compared to those used in the current work (e.g., histology, immunohistochemistry, and other imaging techniques). An epidemiological deliberate maximization of the dehydration exposure analysis based on a large sample is also essential to statistically highlight the correlation between the presence of the sign and the three different types of death identified.

The current study has some limitations, primarily the anatomical differences between human and sheep eyes, as well as differences in their hydration models This factor mainly impacted the timing of the sign's formation but did not prevent the sign from manifesting in all cases. The second limitation affects the morphology and locations of PDSS appearance. In this case, the differences from what is observed in humans are partly due to the anatomical and functional differences between the species but are largely due to the maximization of the ocular surface where dehydration was induced. The third limitation is the small sample size. This was partly due to the limited literature available on tache noire, making it impossible to conduct a preliminary sample size calculation. However, this limitation is somewhat mitigated by the robustness and consistency of the results obtained. The fourth limitation is that in all cases, death was due to hemorrhagic shock. However, this limitation also serves to confirm that deaths from hemorrhagic shock represent a type of death where choroidal detachment occurs, and PDSSs can manifest macroscopically. The decision to select animals that died from a single cause did not compromise the results. Future retrospective epidemiological studies may evaluate whether models involving death from different causes yield similar effectiveness in obtaining the manifestation of PDSSs.

5. Conclusions

The experimental data confirm that the created model, despite some limitations, successfully reproduces PDSSs in all samples where the protocol was applied. The application of this model could lead to a better understanding of PDSSs, particularly in forensic investigations, and inform future research on postmortem ocular changes.

Author Contributions: Conceptualization, M.N., P.E.N., M.F. and E.d.; methodology, M.N., P.E.N., M.F. and E.d.; software, P.E.N. and M.N.; formal analysis, M.N., P.E.N., M.F. and E.d.; investigation, M.N., P.E.N., A.C. and D.N.; resources, E.d. and M.F.; data curation, M.N., P.E.N., A.C. and D.N.; writing—original draft preparation, M.N., P.E.N. and D.N.; writing—review and editing, M.F. and E.d.; visualization, M.N., P.E.N., D.N., A.C., M.F. and E.d.; supervision, E.d. and M.F.; funding acquisition, E.d. and M.F. All authors have read and agreed to the published version of the manuscript.

Funding: This research received no external funding.

Institutional Review Board Statement: Not applicable. This article does not include any studies involving human participants conducted by the authors. Since sheep heads are considered waste material, no specific animal protocol was required, and there were no associated costs.

Informed Consent Statement: Not applicable.

Data Availability Statement: The data presented in this study are available on request from the corresponding author (M.N.).

Acknowledgments: The authors thank Elia Porru, Luca Natali, and Roberto Caria for their contributions to the preliminary studies that were essential for the creation of the model.

Conflicts of Interest: The authors declare no conflicts of interest.

References

1. Sommer, A.G. *Dissertationis de Signis, Mortem Hominis Absolutam Ante Putredinis Accessum Indicantibus, Particula Prior [at Posterior]*; Forbes, J., Conolly, J., Eds.; n.p.: Copenhagen, Denmark, 1833; p. 277.
2. Forbes, J.; Conolly, J. Sommer on the signs of death. In *British and Foreign Medical Review*; Sherwood Gilbert and Piper: London, UK, 1837; Volume IV.
3. Madea, B.; Henssge, C.; Reibe, S.; Tsokos, M.; Kernbach-Wighton, G. Postmortem changes and time since death. In *Handbook of Forensic Medicine*; John Wiley & Sons: Hoboken, NJ, USA, 2014; pp. 75–133. [CrossRef]
4. Madea, B.; Dettmeyer, R.; Schmidt, P. Thanatologie. In *Praxis Rechtsmedizin*; Springer: Berlin/Heidelberg, Germany, 2007; pp. 7–82. [CrossRef]
5. Byard, R.W. Pekka Saukko, Bernard Knight: Knight's forensic pathology 4th ed. *Forensic. Sci. Med. Pathol.* **2018**, *14*, 147. [CrossRef]
6. DiMaio, D.; DiMaio, V.J. *Time of death In Forensic Pathology*, 2nd ed.; CRC Press: London, UK, 2001; pp. 35–36. [CrossRef]
7. DiMaio, V.J.; Molina, D.K. *Postmortem Changes, Time of Death and Identification In DiMaio's Forensic Pathology*; CRC Press: Boca Raton, FL, USA, 2021. [CrossRef]
8. Nioi, M.; Napoli, P.E.; d'Aloja, E.; Nieddu, D.; Chighine, A.; Fossarello, M.; Demontis, R. Postmortal Dark Scleral Spots: Results from a study of 905 cases from a single Institution. *Investig. Ophthalmol. Vis. Sci.* **2023**, *64*, 4768.
9. Napoli, P.E.; Fossarello, M.; d'Aloja, E.; Demontis, R.; Galantuomo, M.S.; Tatti, F.; Nioi, M. Morphological analysis of dark scleral spots by OCT: A preliminary study in human and animal model during the early post-mortem period. *Investig. Ophthalmol. Vis. Sci.* **2023**, *64*, 3395.
10. Nioi, M.; Napoli, P.E.; Demontis, R.; Locci, E.; Fossarello, M.; d'Aloja, E. Postmortem ocular findings in the optical coherence tomography era: A proof of concept study based on six forensic cases. *Diagnostics* **2021**, *11*, 413. [CrossRef]
11. Schrader, S.; Mircheff, A.K.; Geerling, G. Animal models of dry eye. *Surg. Dry Eye* **2008**, *41*, 298–312.
12. Saripalle, S.K.; Schurg, J.; Ross, A. Post-mortem iris biometric analysis in Sus scrofa domesticus. In Proceedings of the 2015 IEEE 7th International Conference on Biometrics Theory, Applications and Systems (BTAS), Arlington, VA, USA, 8–11 September 2015; IEEE: New York, NY, USA, 2015; pp. 1–6.
13. Grieve, K.; Ghoubay, D.; Georgeon, C.; Thouvenin, O.; Bouheraoua, N.; Paques, M.; Borderie, V.; Labbé, A. Stromal striae: A new insight into corneal physiology and mechanics. *Sci. Rep.* **2017**, *7*, 13584. [CrossRef] [PubMed]
14. Iwata, T.; Tomarev, S. Animal models for eye diseases and therapeutics. In *Sourcebook of Models for Biomedical Research*; Conn, P.M., Ed.; Humana Press: Totowa, NJ, USA, 2008; pp. 279–287. [CrossRef]
15. Williams, K.A.; Standfield, S.D.; Mills, R.A.D.; Takano, T.; Larkin, D.F.P.; Krishnan, R.; Russ, G.R.; Coster, D.J. A new model of orthotopic penetrating corneal transplantation in the sheep: Graft survival, phenotypes of graft-infiltrating cells and local cytokine production. *Aust. N. Z. J. Ophthalmol.* **1999**, *27*, 127–135. [CrossRef]
16. Greene, C.A.; Paterson, C.A.; Cook, C.S.; McClure, J.R.; Coats, D.K.; Miller, J.R.; Bossy, C.L.; Beuerman, R.W.; Patel, S. The sheep cornea: Structural and clinical characteristics. *Curr. Eye Res.* **2018**, *43*, 1432–1438. [CrossRef]
17. Isaacson, G.; Wulc, A.E. Applicability of a sheep model for training in plastic surgery of eyelids and orbit. *Ear Nose Throat J.* **2022**, *101*, 43S–49S. [CrossRef] [PubMed]
18. Banstola, A.; Reynolds, J.N. The sheep as a large animal model for the investigation and treatment of human disorders. *Biology* **2022**, *11*, 1251. [CrossRef] [PubMed]
19. Piggins, D.; Phillips, C.J.C. The eye of the domesticated sheep with implications for vision. *Anim. Sci.* **1996**, *62*, 301–308. [CrossRef]
20. Gogola, A.; Jan, N.J.; Lathrop, K.L.; Sigal, I.A. Radial and circumferential collagen fibers are a feature of the peripapillary sclera of human, monkey, pig, cow, goat, and sheep. *Investig. Ophthalmol. Vis. Sci.* **2018**, *59*, 4763–4774. [CrossRef]
21. Caspar, K.R.; Hüttner, L.; Begall, S. Scleral appearance is not a correlate of domestication in mammals. *Zool. Lett.* **2023**, *9*, 12. [CrossRef]
22. Pavel, R.; Ene, I.; Costea, R. Exploring lacrimal gland tear production in sheep under general anesthesia: Examining the potential impact of utilizing 1% hyaluronic acid ophthalmic gel. *Life* **2024**, *14*, 1038. [CrossRef]
23. Creveling, C.J.; Colter, J.; Coats, B. Changes in vitreoretinal adhesion with age and region in human and sheep eyes. *Front. Bioeng. Biotechnol.* **2018**, *6*, 153. [CrossRef]

24. Napoli, P.E.; Nioi, M.; d'Aloja, E.; Fossarello, M. Post-mortem corneal thickness measurements with a portable optical coherence tomography system: A reliability study. *Sci. Rep.* **2016**, *6*, 30428. [CrossRef]
25. Nioi, M.; Napoli, P.E.; Demontis, R.; Locci, E.; Fossarello, M.; d'Aloja, E. Morphological analysis of corneal findings modifications after death: A preliminary OCT study on an animal model. *Exp. Eye Res.* **2018**, *169*, 20–27. [CrossRef]
26. Napoli, P.E.; Nioi, M.; Gabiati, L.; Laurenzo, M.; De-Giorgio, F.; Scorcia, V.; Grassi, S.; d'Aloja, E.; Fossarello, M. Repeatability and reproducibility of post-mortem central corneal thickness measurements using a portable optical coherence tomography system in humans: A prospective multicenter study. *Sci. Rep.* **2020**, *10*, 14508. [CrossRef]
27. Nioi, M.; Napoli, P.E.; Demontis, R.; Chighine, A.; De-Giorgio, F.; Grassi, S.; Scorcia, V.; Fossarello, M.; d'Aloja, E. The influence of eyelid position and environmental conditions on the corneal changes in early postmortem interval: A prospective, multicentric OCT study. *Diagnostics* **2022**, *12*, 2169. [CrossRef]
28. Locci, E.; Stocchero, M.; Gottardo, R.; Chighine, A.; De-Giorgio, F.; Ferino, G.; Nioi, M.; Demontis, R.; Tagliaro, F.; d'Aloja, E. PMI estimation through metabolomics and potassium analysis on animal vitreous humour. *Int. J. Legal Med.* **2023**, *137*, 887–895. [CrossRef]
29. Rosa, M.F.; Scano, P.; Noto, A.; Nioi, M.; Sanna, R.; Paribello, F.; De-Giorgio, F.; Locci, E.; d'Aloja, E. Monitoring the modifications of the vitreous humor metabolite profile after death: An animal model. *BioMed Res. Int.* **2015**, *2015*, 627201. [CrossRef]
30. Locci, E.; Stocchero, M.; Gottardo, R.; De-Giorgio, F.; Demontis, R.; Nioi, M.; Chighine, A.; Tagliaro, F.; d'Aloja, E. Comparative use of aqueous humour 1H NMR metabolomics and potassium concentration for PMI estimation in an animal model. *Int. J. Legal Med.* **2021**, *135*, 845–852. [CrossRef]
31. Šoša, I. Ocular Surface Fluid: More than a Matrix. *Toxics* **2024**, *12*, 513. [CrossRef]
32. Cher, I. Fluids of the ocular surface: Concepts, functions and physics. *Clin. Exp. Ophthalmol.* **2012**, *40*, 634–643. [CrossRef]
33. Napoli, P.E.; Nioi, M.; Mangoni, L.; Gentile, P.; Braghiroli, M.; d'Aloja, E.; Fossarello, M. Fourier-Domain OCT Imaging of the Ocular Surface and Tear Film Dynamics: A Review of the State of the Art and an Integrative Model of the Tear Behavior during the Inter-Blink Period and Visual Fixation. *J. Clin. Med.* **2020**, *9*, 668. [CrossRef]